BIPERIODIC ACCELERATING STRUCTURE WITH INNER COUPLING CELLS WITH AN INCREASED COUPLING COEFFICIENT

M.A. Gusarova, I.I. Petrushina, E.A. Savin, N.P. Sobenin, National Research Nuclear University «MEPhI», Moscow, Russia

Abstract

In this article the research results of advanced biperiodic accelerating structure (BAS) re presented. This structure features increased coupling coefficient together with keeping of effective shunt impedance high value and another electrodynamics parameters.

ELECTRODYNAMICS CHARACTERISTICS

In order to characterize of accelerating cavity efficiency for low current case the effective shunt impedance per unit length is commonly used:

$$r_{\text{sh.ef}} = \left| \int_0^l E_z(z) \exp(ik_z z) dz \right|^2 \Big/ \left(P_{\text{loss}} l\right). \quad (1)$$

where $\dot{E}_z(z)$ – accelerating field electric complex amplitude; l– cavity length; P_{loss} – power losses, k_z – wave number in the z direction.

One of the most important electrodynamics characteristics for accelerating cavities is Q-factor

$$Q = 2\pi \frac{W_{stor}}{(W_{scat.res})_{T_0}} = \omega_0 \frac{W_{stor}}{P_{scat.res}}. \quad (2)$$

where W_{stor} – stored energy in magnetic end electric fields in cavity

$(W_{scat.res})_{T_0} = P_{scat.res} \cdot T_0$ – scattered energy in cavity during oscillations period, $P_{scat.res}$ – scattered power in active resistance at resonance.

Last parameter worth to be mentioned is coupling coefficient. It is defined by ratio of frequencies of π, π/2 and 0 modes

$$k = \frac{|f_\pi - f_0|}{f_{\pi/2}}. \quad (3)$$

SIMULATION MODEL

Model used for numeric simulation consists of two accelerating cells and one coupling cell between them. On Fig.1 illustrates this model with geometry parameters shown.

CALCULATION PROCESS

Each type of BAS design has been optimized on π/2 mode operating frequency both for accelerating and coupling cells.

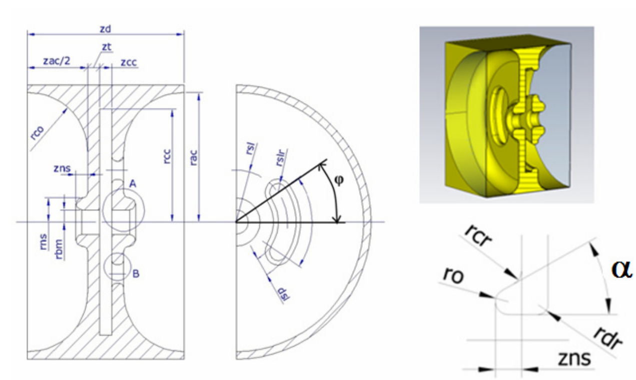

Figure 1: Structure geometry.

During researching in order to increase coupling for BAS design with inner coupling cells dual LINAC geometry was used [2]. Accelerating structure of this LINAC is designed to operate at 2856 MHz. Maximum value of coupling coefficient in accelerating section of this LINAC (with wave phase velocity equal to the 0.999c) became 10.3% instead of original 5% [1].

During the cavity optimization the following parameters remained invariable: beam pipe radius rbm, structure period zd, coupling gap thickness zt, coupling cell length zcc. The electrodynamic characteristics dependence of coupling gap radial position rsl, coupling gap width dsl, accelerating cell equator rounding rco were studied.

SWEEPING OF ACCELERATING CELL EQUATOR RADIUS

With increasing of accelerating cell equator rounding (rco) values of shunt impedance and Q-factor are increased. But this geometry change leads to coupling slots displacement – they are no longer in the maximum magnetic field region in accelerating cells and coupling cell. This results in coupling coefficient drop.

SWEEPING INNER COUPLING CELLS THICKNESS

With increasing of coupling gap thickness dsl from 9 to 13 mm angular size of coupling gap φ must be reduced from 30^0 to 25^0 to avoid coupling gaps overlapping.

In the same way radius of coupling gap middle line rsl must be reduced from 21.4 mm to 19.82 mm to place coupling gap as close to accelerating cell blend edge that leads to coupling coefficient

Copyright © 2012 by the respective authors — cc Creative Commons Attribution 3.0 (CC BY 3.0)

ISBN 978-3-95450-125-0

EXPANSION OF COUPLING CELL IN BEAM PIPE AREA

The coupling cell length zcc is expanded in the area close to cavity axis (Fig2). Simultaneously the zac/2-zns dimension is reduced by the same value t.

Cavity radius Rc was changed to place coupling slot as close to accelerating cell equator as possible while optimizing coupling cell geometry.

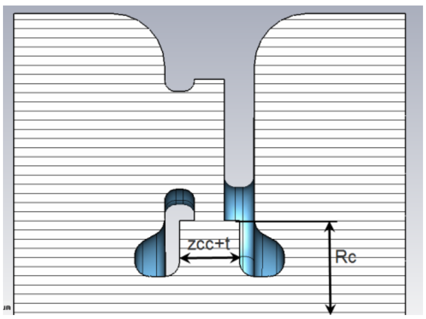

Figure 2: Coupling cell expansion.

Electrodynamic characteristics dependence on coupling gap thickness dsl for such structure geometry was studied. With dsl increase from 7 to 13 mm angular size of coupling gap φ must be reduced from 35^0 to 25^0 to avoid coupling gaps overlapping. In the same way coupling gap radial location rsl must be reduced from 25.25 mm to 23.22 mm to place coupling gap as close to accelerating cell equator as possible. This leads to coupling coefficient drop.

The structure with magnetic coupling increased by reducing diaphragm thickness zt in the coupling gaps region is the modification of geometry where coupling cell in axis region lengthened.

Rc radius value was changed while optimizing coupling cell geometry in order to place coupling gap as close to accelerating cell equator where magnetic field is maximal.

For this geometry with the following sizes: dsl=13mm, t=3.8mm, rco=7mm,φ=25^0,zt=2mm, (rcslr=1mm) with Rc value equal to 11.98 mm the coupling coefficient k=15,87% was obtained at $r_{sh.ef.}$ =80,8 MOhm/m, Q=16090, $E_{max}/E_{acc.}$=3,2.

Coupling coefficient for the model considered can be increased up to 19% by making recess in coupling gap area at the accelerating cell side (Fig 3). In the same way the effective shunt impedance will be reduced to 76 MOhm/m and Q-factor will be reduced to 14100.

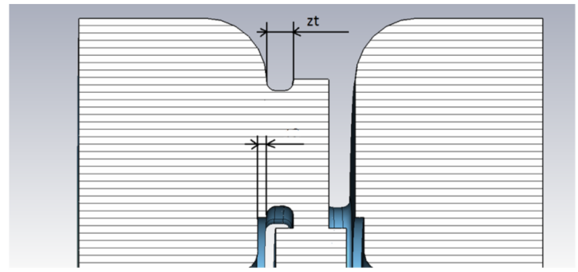

Figure 3: Coupling window recess.

ADJUSTMENT OF BEAM PIPE GEOMETRY

The coupling coefficient increases with zns rise because electrical field coupling drop. The value of effective shunt impedance has an optimum at zns=5.8 mm. The E_{max}/E_{acc} ratio increases from 3.4 to 4.5 at zns increasing in the same range.

MULTIPACTING SIMULATIONS

The electrical strength is important for the RF structure operation. Multipactor discharge is dangerous and goes along with the RF (or high-frequency) breakdown. Multipacting occurs at low levels of the electric field and is located in the coupling cells and in the areas that are close to the surface of a structure [3].

Multipacting simulations were done for four structures of the BAS with various modifications mentioned above.

The special code for multipacting simulations Multp-M was used [4].The dependence of secondary particle number vs. accelerating gradient in a wide range of latter is shown in Fig. 4.

The trajectories of the particle motion were investigated at different levels of the accelerating gradient. Multipactor trajectories were observed:

- on iris close to beam pipe from accelerating cell side (Fig. 5a) at low field strength;

Table 1: Comparison of the Results

№	1	2	3	4
$f_{p/2}$, MHz	2856.01	2855.99	2856.01	2855.94
f_{couple}, MHz	2855.96	2856	2856.01	2855.94
k,%	13	15.5	15.87	19.2
$\lvert B_{gr}\rvert$,%	19.5	22.4	22.5	26.9
$r_{sh.ef.}$, MOhm/m	81.67	76.77	80.8	75.84
T	0.81	0.81	0.77	0.81
Q	15811	15049	16088	14075
$r_{sh.ef.}$/Q, Ohm/m	5165	5101	5022	5388
E_{acc}, MV/m	51.3	50.1	53.3	52.9
E_{max}/E_{acc}	3.21	3.46	3.2	4.14
H_{max} , MA/m	0.256	0.332	0.347	0.44

ISBN 978-3-95450-125-0

Copyright © 2012 by the respective authors — cc Creative Commons Attribution 3.0 (CC BY 3.0)

- in equator areas of the coupling cell (Fig. 5b)
- on accelerating cell equator at the electric field strength levels above 9 MV/m (Fig. 5c)

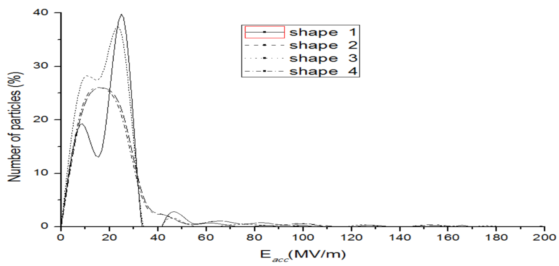

Figure 4: The number of secondary electrons in the cavity as a function of the accelerating gradient (0-200 MV/m).

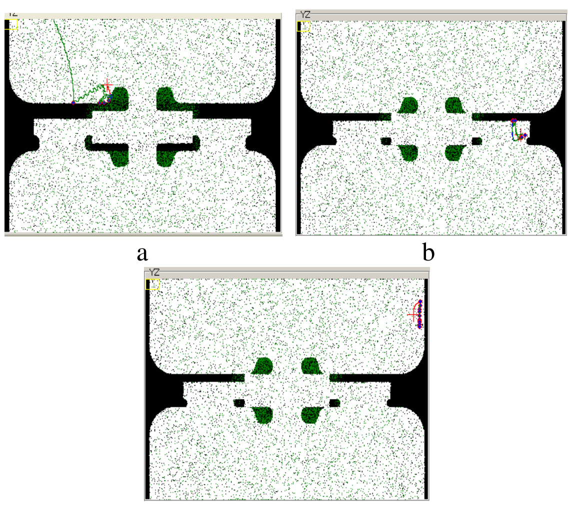

Figure 5: Electron trajectories in the structure at different levels of the accelerating gradient.

The results of the trajectory stability investigations in various areas of the structures are shown in Table 2.

Table 2: The results of the trajectory stability investigations in various areas of the structures: on beam pipe to iris connection area (a); in coupling cell (b); on accelerating cell equator (c).

№	a	b	c
1	~ 1.6 MV/m unstable	3–20 MV/m stable	7-20 MV/m stable
2	~0.8 MV/m stable	~ 12 MB/м stable	4.8 – 6.5 MV/m (on the blending part) stable 13.8 – 20 MV/m stable
3	1.3-2.3 MV/m stable	8 -13.8 MV/m stable	5-10 MV/m (on the blending part) stable 10 – 20 MV/m stable
4	~1 MV/m stable	5.5 – 12 MV/m stable	~15 MV/m stable

Thus, the simulation results show that:

- The first modification of the BAS with the standard coupling cell undergoes the multipacting most of all. It is obvious because the smaller the gap, the higher probability of the multipactor discharge;
- Trajectories in the coupling cell are of high order multipactor trajectories (10th and above), they are strongly twisted (curly). Electrons following these trajectories have a low probability to reach the opposite cavity wall. Consequently, such trajectories are not dangerous;
- Most of the stable trajectories are observed in accelerating cell. The motion of the particles can be described as "sliding" along the wall. The mostly apparent trajectories of this type occur in the structure shape 3.

CONCLUSION

Results of four preferred geometry types studies are given in Table 1. Geometry types are described below: 1.Geometry shown on Fig1; 2.The structure with coupling cell expansion in connection with the beam pipe area; 3.The structure with coupling cell expansion and shorter coupling cell because of expanded accelerating cell; 4. The structure with coupling cell expansion and shorter coupling cell with coupling window recess (Fig 2).

The results of multipacting simulations showed that the structure (1) undergoes the Multipactor discharge most of all. Stable trajectories were observed in areas of the coupling cell and on the walls of the accelerating cell in the range of the accelerating gradient of about 5-20 MV/m.

REFERENCES

[1] O.A.Valdner, N.P.Sobenin, at. al., "The directory about diaphragm loaded waveguides", Energoatomizdat, 1991
[2] A.A. Zavadtsev, N.P.Sobenin, et. al., "The system for cargo inspection based on dual LINAC", Devices and experimental techniques, 2011, №2, p 1-9.
[3] Paramonov V., Tarasov S, "The possibility of multipactor discharge in coupling cells of coupled-cells accelerating structures", 1998 Linac Conference, Chicago, 1998.
[4] M.A. Gusarova, S.V. Kutsaev, V.I. Kaminsky, "Multipacting simulation in accelerator RF structure", Nuclear Instrument and Methods in Physics Research A, 599. P. 100-105, 2009

Copyright © 2012 by the respective authors — cc Creative Commons Attribution 3.0 (CC BY 3.0)

ISBN 978-3-95450-125-0